

# Assessing the accuracy of quantum Monte Carlo and density functional theory for energetics of small water clusters

M. J. Gillan<sup>1,2,3</sup>, F. R. Manby<sup>5</sup>, M. D. Towler<sup>4,6,7</sup> and D. Alfè<sup>1,2,3,4</sup>

<sup>1</sup>London Centre for Nanotechnology, Gordon St, London WC1H 0AH, UK

<sup>2</sup>Dept of Physics and Astronomy, UCL, Gower St, London WC1E 6BT, UK

<sup>3</sup>Thomas Young Centre, UCL, Gordon St, London WC1H 0AH, UK

<sup>4</sup>Dept of Earth Sciences, UCL, Gower St, London WC1E 6BT, UK

<sup>5</sup>Centre for Computational Chemistry, School of Chemistry, University of Bristol,  
Bristol BS8 1TS, UK

<sup>6</sup>TCM Group, Cavendish Laboratory, University of Cambridge,  
Madingley Rd, Cambridge CB3 0HE, UK

<sup>7</sup>Apuan Alps Centre for Physics, via del Collegio 22, Vallico Sotto  
Fabbriche di Vallico 55020, Italy

October 10, 2018

## Abstract

We present a detailed study of the energetics of water clusters  $(\text{H}_2\text{O})_n$  with  $n \leq 6$ , comparing diffusion Monte Carlo (DMC) and approximate density functional theory (DFT) with well converged coupled-cluster benchmarks. We use the many-body decomposition of the total energy to classify the errors of DMC and DFT into 1-body, 2-body and beyond-2-body components. Using both equilibrium cluster configurations and thermal ensembles of configurations, we find DMC to be uniformly much more accurate than DFT, partly because some of the approximate functionals give poor 1-body distortion energies. Even when these are corrected, DFT remains considerably less accurate than DMC. When both 1- and 2-body errors of DFT are corrected, some functionals compete in accuracy with DMC; however, other functionals remain worse, showing that they suffer from significant beyond-2-body errors. Combining the evidence presented here with the recently demonstrated high accuracy of DMC for ice structures, we suggest how DMC can now be used to provide benchmarks for larger clusters and for bulk liquid water.

# 1 Introduction

Water in its many forms is one of the most intensively studied of all substances, because of its relevance to so many different scientific and technological fields. But in spite of many decades of effort, a fully comprehensive account of the energetics of water systems at the molecular level is still lacking. Density functional theory (DFT) is very important in water studies, since it is readily applied to the bulk liquid [1, 2, 3, 4] and solid [5, 6, 7, 8] and their surfaces [9, 10], as well as to solutions [11, 12], and to interfaces with other materials [13, 14]. Unfortunately, DFT does not yet give satisfactory overall accuracy [15, 16, 17, 18, 19, 20, 21], and the past few years have seen strenuous efforts to analyse and remedy the deficiencies of current DFT approximations [22, 23, 24]. Wavefunction-based molecular quantum chemistry techniques, particularly MP2 (second-order Møller-Plesset) and CCSD(T) (coupled-cluster singles and doubles with perturbative triples), the latter often referred to as the “gold standard”, can reliably deliver much higher accuracy than DFT. These quantum chemistry techniques have been extensively used to study water clusters [25, 26, 27, 28, 29, 30, 31, 32, 33, 34, 35, 36, 37, 38] and to develop parameterised interaction models [39, 40, 41, 42, 43, 44, 45, 46, 47, 48, 49, 50]. However, the cost of obtaining this high accuracy increases dramatically with system size. The direct application of correlated quantum chemistry methods to bulk solid and liquid water is still in its infancy [51, 52]. Recently, quantum Monte Carlo (QMC) methods, and in particular diffusion Monte Carlo (DMC) [53, 54, 55, 56, 57] have begun to be applied to both cluster and bulk forms of water [23, 60, 61] and the results indicate that DMC is much more accurate than DFT for these systems as well as for weak non-covalent interactions in other molecular systems [62, 63]. Our purpose in this paper is to present a systematic comparison of the accuracy of DMC and DFT approximations for a wide range of configurations of small H<sub>2</sub>O clusters, ranging from the monomer to the hexamer. The use of thermal ensembles of configurations and the many-body analysis of errors in the total energy are important themes of the work.

The errors of DFT are already troublesome for the H<sub>2</sub>O monomer, and it has been shown recently [64] that some common exchange-correlation functionals give rather poor accuracy for its distortion energy, underestimating the O-H bond-stretch energy. Difficulties with the energetics of the dimer are well known [26, 65], with concerns about short-range exchange-repulsion and intermediate-range hydrogen bonding, as well as the lack of long-range dispersion in standard forms of DFT. Many-body interactions are also known to play an important role in water energetics [25, 27, 45, 47, 48, 49, 66, 67], with induction effects due to the dipolar and higher multipolar polarisabilities of the monomer generally regarded as the dominant contribution, so that inaccurate DFT predictions of these polarisabilities may be problematic. In order to describe the subtle balance between these different interaction mechanisms without adjustment of empirical parameters, a good description of all of them is highly desirable.

The many-body expansion of the total energy of a system of molecules gives a helpful way of analysing the different types of interaction in water [25, 27, 66], and has also played a key role in the construction of interaction

models fitted to molecular quantum chemistry calculations [50]. In this expansion, the total energy of a system of  $N$  molecules is expressed as

$$E = E^{(1)} + E^{(2)} + E^{(3)} + \dots, \quad (1)$$

where

$$\begin{aligned} E^{(1)} &= \sum_i E(i), \\ E^{(2)} &= \sum_{i < j} \delta E(i, j), \\ E^{(3)} &= \sum_{i < j < k} \delta E(i, j, k), \end{aligned}$$

etc. Throughout the paper we use the notation  $E(1, 2, \dots)$  to denote the energy of the system composed of the listed monomers, and the 2- and 3-body energy increments are given by the usual formulae:

$$\begin{aligned} \delta E(i, j) &= E(i, j) - E(i) - E(j) \\ \delta E(i, j, k) &= E(i, j, k) - \delta E(i, j) - \delta E(i, k) - \delta E(j, k) - E(i) - E(j) - E(k). \end{aligned} \quad (2)$$

We use the notation  $E^{(>2)}$  to denote all of the beyond-2-body effects, i.e.  $E^{(>2)} = E - E^{(1)} - E^{(2)}$ .

By calculating the DMC energy for sets of configurations of H<sub>2</sub>O clusters from the monomer to the hexamer, and by comparing these energies with many-body decompositions of both benchmark CCSD(T) energies and of energies given by various DFT approximations, we will attempt to probe the accuracy of DMC for the 1-, 2- and beyond-2-body parts of the energy. The evidence to be presented will indicate that DMC is very accurate for all the main components of the energy, while the DFT approximations we study all encounter difficulties with one or more of them. An important feature of this work is that many of our configuration sets are random statistical samples created by drawing clusters from a classical simulation of liquid water based on an interaction model for flexible monomers. A recent investigation of monomer and dimer energetics was based on a similar idea [64].

Our work builds on very extensive earlier work on water clusters in which DFT has been compared with accurate molecular quantum chemistry calculations [32, 34, 36, 61, 64, 69, 70, 71], sometimes employing the many-body expansion, though rather little of that work has been done on the kind of random statistical samples that we emphasise here. We also build on previous DMC work on clusters [60, 61], bulk water [80] and ice structures [23]. The DMC work already reported on clusters [60, 61] investigated only a single configuration of the dimer and some of the equilibrium isomers of the hexamer, but was vital in giving evidence for the accuracy of DMC for water systems. Very recent work on the cohesive energy and relative energies, equilibrium volumes and transition pressures of a number of ice structures [23] demonstrated the remarkable accuracy of DMC ( $\sim 0.2 \text{ m}E_h \simeq 5 \text{ meV}$  per monomer) in the bulk. Combining the evidence from that work on ice with the present evidence on clusters, we shall argue that DMC can now be regarded as a valuable tool which will be able to provide benchmark energies for larger clusters, for statistical samples of configurations of liquid water under a range of conditions, and for more complex systems such as ice surfaces.

## 2 Techniques

Quantum Monte Carlo methods have been described in detail in many previous papers [53, 54, 55, 56, 57, 58, 59]. The main technique used here is diffusion Monte Carlo (DMC), which is a stochastic technique for obtaining the ground-state energy of a general many-electron system. We recall that it works by propagating an initial trial many-electron wavefunction in imaginary time, with the time-dependent part of the wavefunction represented by an evolving population of walkers. Although DMC is in principle exact, practical calculations generally employ the fixed-node approximation [72] and the pseudopotential locality [73] approximation. Errors arising from both these approximations are greatly reduced by improving the accuracy of the trial wavefunction, and we do this by variance minimisation [74] within variational Monte Carlo. (The alternative procedure of energy minimisation is favoured by some research groups.) All our DMC calculations are made with the CASINO code [75].

We use conventional Slater-Jastrow wavefunctions with a Jastrow factor containing electron-nucleus, electron-electron and electron-nucleus-electron terms, each of which depends on variational parameters [76]. We use Dirac-Fock pseudopotentials [77], with the oxygen pseudopotential having a He core with core radius 0.4 Å and the hydrogen pseudopotential having core radius 0.26 Å. The single-electron orbitals in the trial wavefunction are obtained from plane-wave LDA calculations performed with the PWSCF code [78]. We use LDA to generate the single-electron orbitals, because the evidence indicates that this usually gives more accurate many-electron trial functions than other DFT approximations or Hartree-Fock [63]. These DFT calculations are performed on water clusters in large cubic boxes having a length of 40 a.u. in periodic boundary conditions, with  $\Gamma$ -point sampling and a plane-wave cut-off of 300 Ry. The resulting single-electron orbitals are then re-expanded in B-splines [79] and the DMC calculations are performed with free (as opposed to periodic) boundary conditions. The B-spline grid has the natural spacing  $a = \pi/G_{\max}$ , where  $G_{\max}$  is the plane-wave cut-off wavevector.

Since DMC is a stochastic technique, its computed energies suffer from a statistical error, which is inversely proportional to the square root of configuration-space sampling points, so that it is desirable to increase the number of walkers and the imaginary-time duration of the run. Since the recent DMC work on ice structures [23] suggests that DMC is capable of an accuracy of 0.1 – 0.2  $mE_h$ /monomer or better for water systems, we generally aim to run the DMC calculations long enough to reduce the statistical error below this tolerance. For the imaginary-time propagation of DMC, we use a time-step of  $\delta t = 0.005$  a.u. This value was chosen after tests with smaller  $\delta t$  down to 0.001 a.u., which showed that with  $\delta t = 0.005$  a.u. the total energy of the H<sub>2</sub>O monomer is converged to within 0.4  $mE_h$ . This tolerance is outside our target of 0.1  $E_h$  per monomer, but we are concerned in this work with energy *differences*, and we expect that all the relevant differences will be converged with respect to time-step to very much better than 0.4  $mE_h$  with  $\delta t = 0.005$  a.u. Our DMC results on the H<sub>2</sub>O monomer (Sec. 3.1) will confirm this. As further confirmation, we have also made tests on the energy differences between dimer configurations with  $\delta t$  ranging from 0.001 to 0.005 a.u. and we find a variation of no more than 0.1  $mE_h$ .

All the present DMC calculations were performed on the JaguarPF supercomputer at Oak Ridge National Laboratory, which at the time of the calculations consisted of 224,000 cores organised into 12-core shared-memory nodes. The parallel implementation of the CASINO code distributes walkers over cores. Because the walker populations fluctuate, we find that reasonable load-balancing is achieved only if the mean number of walkers on each core is at least 10. The total number of walkers and hence the optimal number of cores depend strongly on the number of atoms in the system and the required statistical accuracy, but in general we find it convenient to use up to about 50,000 cores. The parallel scaling of our CASINO implementation on JaguarPF is excellent, becoming essentially perfect for very large numbers of walkers. For the statistical samples of configurations used in the present work, it is efficient to run a number of DMC calculations simultaneously.

Our absolute standard of accuracy throughout this work is the coupled-cluster approximation CCSD(T) in the complete basis-set (CBS) limit. Of course, this limit cannot be attained, but our convergence criterion is that residual basis-set errors should be less than the threshold of  $0.1 mE_h/\text{monomer}$  mentioned above. In order to achieve this tolerance, we use the identity

$$E(\text{CCSD(T)}) = E(\text{MP2}) + E(\Delta\text{CCSD(T)}) , \quad (3)$$

where  $E(\Delta\text{CCSD(T)}) \equiv E(\text{CCSD(T)}) - E(\text{MP2})$  is the change of the correlation energy when CCSD(T) is used in place of MP2. This allows us to use different basis sets for  $E(\text{MP2})$  and  $E(\Delta\text{CCSD(T)})$ , exploiting the fact that the size of basis set needed to converge  $E(\Delta\text{CCSD(T)})$  is less than that needed to converge  $E(\text{CCSD(T)})$  itself. This approach is sometimes referred to as the ‘‘focal point’’ scheme [31, 81, 82]. All our molecular quantum-chemistry calculations are performed with the MOLPRO code [83, 84].

For all the benchmark calculations, we use the Dunning augmented correlation-consistent basis sets aug-cc-pVXZ [85, 86], with X the cardinality, referred to here simply as AVXZ. The basis-set convergence of Hartree-Fock (HF) energies is rapid and unproblematic, and that of correlation energies can be greatly accelerated by the use of F12 (explicitly correlated) methods [87, 88, 89]. The F12 method is available for both MP2 and CCSD(T) in the MOLPRO code [90, 91], and we use it in all the present calculations. In addition, the efficiency of HF and MP2 calculations, and of F12 contributions to MP2 and CCSD(T), is greatly enhanced by using density fitting (DF) [90, 92, 93, 94], the errors incurred being typically a few  $\mu E_h$ , and so completely negligible for present purposes.

Since the many-body decomposition (Eq. (1)) plays a key role in our analysis, we need the many-body components of the benchmark CCSD(T) energy for every configuration studied. For the 1-body energy  $E^{(1)}$ , rather than using CCSD(T) itself, we prefer to use the more accurate Partridge-Schwenke (PS) energy function [68]. This is an elaborate parameterised function fitted to a very large number of extremely accurate quantum chemistry calculations spanning a wide range of monomer geometries. The function, denoted here by  $E^{(1)}(\text{PS})$ , has been shown to have spectroscopic accuracy, and it can therefore be regarded as essentially exact for present purposes. When we refer to CCSD(T) benchmarks, what we actually mean is  $E^{(1)}(\text{PS}) + E^{(2)}(\text{CCSD(T)}) + \dots$

The many-body decomposition is an additional aid to basis-set convergence, with smaller basis sets sufficing for high-order interaction terms. As a further important point of technique, we systematically use the counterpoise method [95, 96] to reduce basis-set superposition error in all our calculations; so for example to calculate a 2-body energy contribution  $\delta E(i, j) = E(i, j) - E(i) - E(j)$  the full dimer basis sets is used for each of the three contributions. For completeness, we note that we do not include core correlation or relativistic corrections. These corrections were studied for the H<sub>2</sub>O dimer by Tschumper *et al.* [31] and found to be typically a few  $\mu E_h$ .

To conclude our summary of techniques, we note briefly how we have performed the DFT calculations. We use the same Dunning correlation-consistent AVXZ basis sets that we used for the benchmark calculations, and we find that the differences between successive cardinalities decrease in essentially the same way for all the functionals as in the HF calculations, so that convergence of the total energy to our tolerance of 0.1 mE<sub>h</sub>/monomer is easy to achieve. In computing the many-body components of the energy, we use exactly the same counterpoise methods outlined above for the benchmark calculations.

### 3 DMC and DFT compared with benchmarks

We will start by studying a thermal sample of configurations of the H<sub>2</sub>O monomer drawn from a classical molecular dynamics (m.d.) simulation of the bulk liquid based on the flexible AMOEBA model [97, 98]. The comparisons will allow us to assess the accuracy of DMC and DFT approximations for the 1-body energy  $E^{(1)}$ . For the dimer, we will gain insight into the 2-body energy by comparing DMC and DFT energies with benchmarks for two sets of configurations: first, the 10 stationary points which have been extensively studied in earlier work [31, 34, 44, 46, 99]; and second, a thermal sample of 198 configurations drawn from the bulk liquid. We then move on to comparisons for thermal samples of the trimer, tetramer, pentamer and hexamer, which allow us to see how well the different methods account for the beyond-2-body energy  $E^{(>2)}$ . At the end of the Section, we will present results for the many-body decomposition of the energy of a number of stationary points of the hexamer, for which QMC results have been reported in earlier work [61].

Since all our thermal samples of cluster configurations were drawn from the same AMOEBA m.d. simulation, we summarise the relevant details here. Monomer flexibility is one of the important features of the AMOEBA model [97, 98], whose parameters are adjusted to fit selected *ab initio* and experimental data. The model also accounts for many-body interactions through distributed polarisabilities of the monomers. It is known to give a rather good description of the radial distribution functions and the self-diffusion coefficient of liquid water over quite a range of conditions, including ambient. The m.d. simulation run from which we drew the configurations was performed on a system of 216 water molecules in periodic boundary conditions at the ambient density of 1.0 gm/cm<sup>3</sup> and room temperature (300 K). This way of making thermal samples is motivated by our long-term aim of obtaining accurate descriptions of the energetics of condensed phases of water in thermal equilibrium. To this end, it is natural to demand that the methods we use should be accurate for cluster geometries typical

of those found in the condensed phases of interest. Naturally, we have to bear in mind always that the mean and rms errors we find on comparing a chosen technique with benchmark energies for a thermal sample are not absolute quantities, but will depend on the way the sample was constructed.

### 3.1 The monomer

All our calculations on the monomer were performed on a set of 100 configurations drawn at random from the AMOEBA m.d. simulation. The mean value of the O-H bond length in this sample was 0.968 Å, and the probability distribution of bond-lengths was roughly Gaussian, with an rms fluctuation about the mean of 0.019 Å; the minimum and maximum O-H bond lengths occurring in the sample were 0.913 and 1.020 Å. The mean and rms fluctuation of the H-O-H bond angle were 105.3° and 3.7° respectively, with the minimum and maximum angles being 97.0° and 117.0°.

We assess the errors of DMC and DFT approximations for the monomer by comparing their energies with the essentially exact Partridge-Schwenke energy function  $E^{(1)}(\text{PS})$  referred to in Sec. 2. The equilibrium monomer geometry according to PS has bond lengths of 0.95865 Å and a bond angle of 104.348°. It is convenient to take this as the “standard” geometry of the isolated monomer, so that when we refer to the energy of the monomer in any geometry computed with a given method we will always mean the energy of that geometry minus the energy in the PS equilibrium geometry computed with the same method. This means that the monomer energy with PS itself is by definition non-negative, but with a DFT approximation or with DMC it can be negative, since the minimum-energy configurations with these methods will generally differ from the PS equilibrium geometry.

Our DMC calculations on the 100 monomer configurations were performed as described in Sec. 2. In our production results, the Jastrow factor was not re-optimised for each geometry. We used a smaller set of 25 configurations to test the effect of re-optimising it, and we could not detect any significant changes of energy due to re-optimisation. For every geometry, the DMC calculations were continued long enough to reduce the rms statistical errors to 30  $\mu E_h$ . We show in Fig. 1  $E(\text{DMC}) - E(\text{PS})$  plotted against  $E(\text{PS})$ . The distortion energy itself covers a range up to  $\sim 5 mE_h$  (140 meV), and we see that DMC errors are only a tiny fraction of this. In fact, for the given thermal sample, the mean DMC error and its rms fluctuation about the mean are 10 and 40  $\mu E_h$  (Table 1).

We have made comparisons against PS also for DFT, using the PBE, BLYP, B3LYP and PBE0 exchange-correlation functionals and the AV5Z basis. Our convergence tests using AVQZ indicate mean (rms) errors due to basis-set incompleteness of around 4 (10)  $\mu E_h$  for all functionals, suggesting that any residual basis-set errors beyond AV5Z will be much smaller than 10  $\mu E_h$  (0.27 meV).

The differences  $E(\text{DFT}) - E(\text{PS})$  are also displayed in Fig. 1, and the mean and rms fluctuations are recorded in Table 1. We see from this that PBE and BLYP give very poor results, and their negative deviations from the PS benchmarks imply that the energy needed to distort the monomer is considerably underestimated by

both approximations, as already noted in a recent paper by Santra *et al.* [64]. The B3LYP functional is much better, but PBE0 is the clear winner out of the functionals examined, with mean and rms errors of only  $-10$  and  $80 \mu E_h$ . The good performance of PBE0 for the monomer was also reported by Santra *et al.* [64]. However, DMC is markedly superior, and it appears that residual DMC errors in the 1-body energy can safely be neglected in cluster and bulk systems, at least so long as the variation of the bond lengths and bond angle are not too much larger than those treated here.

## 3.2 The dimer

### 3.2.1 The stationary points

The geometries of the 10 dimer stationary points are depicted in many previous papers (see e.g. Ref. [31]), and there is a standard numbering, which we follow here. We have worked with two closely related sets of configurations for the stationary points. The configurations of Tschumper *et al.* [31] were used for the tests we performed to check that our techniques can deliver dimer energies with CCSD(T) within  $100 \mu E_h$  of the CBS limit. However, because of the way the project developed, the DMC and DFT calculations were performed on a slightly different configuration set due to the Bowman group [46], and we used exactly the same techniques tested on the Tschumper set to produce our CCSD(T) benchmarks for the Bowman set.

Our benchmarks for the total dimer energy are represented as

$$E = E^{(1)}(\text{PS}) + E^{(2)}(\text{MP2-F12/AV5Z}) + E^{(2)}(\Delta\text{CCSD(T)-F12/AVQZ}) \quad (4)$$

with full counterpoise for all energies. Our basis-set tests show that with AVQZ the HF and MP2-F12 correlation energies have residual basis-set errors of less than  $\sim 15$  and  $\sim 10 \mu E_h$  respectively, while with AVTZ the basis-set errors in  $E^{(2)}(\Delta\text{CCSD(T)} - \text{F12})$  are less than  $\sim 30 \mu E_h$ . For the present calculations on the stationary points, we have gone beyond this so that the remaining basis-set errors should be much less than those just quoted, and our comparisons with the energies reported by Tschumper *et al.* confirm this.

Our DMC calculations on the total energies of the stationary points are computed as described in Sec. 2. The runs were continued long enough to reduce the DMC statistical error to  $77 \mu E_h$ . Since we focus here on the energies of the stationary points relative to that of the global minimum, we have extended the run on the global minimum so that its rms statistical error is only  $44 \mu E_h$ . The relative DMC energies are compared with the CCSD(T) benchmarks in Table 2, and we see that they agree in all but two cases within better than  $100 \mu E_h$  ( $2.7 \text{ meV}$ ), and in those two cases the DMC errors are still less than  $170 \mu E_h$ .

We already know from earlier work [34] that DFT predictions of the energies of the stationary points suffer from much larger errors than the DMC errors just mentioned, but we considered it worthwhile to calculate our own values using PBE, BLYP, B3LYP and PBE0. (We note that the present DFT energies are all calculated at exactly the same geometries, rather than at the stationary-point geometries that would be given by the DFTs



themselves, and this should be borne in mind when comparing with earlier DFT results.) Our tests of basis-set convergence for DFT show that with AV5Z the relative energies of the stationary points are converged to better than  $20 \mu E_h$ . We report values of these relative energies for the Bowman geometries in Table 2. We see that the DFT approximations overestimate all the energy differences between the stationary points and the global minimum, with many of the DFT errors being greater than  $0.5 mE_h$  and a few being as much as  $1.0 mE_h$ , in general agreement with earlier work [34]. The hybrid functionals B3LYP and PBE0 perform slightly better than non-hybrid PBE and BLYP, but there is not a great deal to choose between them. The individual monomers have almost exactly the same geometries at the 10 stationary points, so that DFT errors in the monomer distortion energies play almost no role here, and any disagreements with the benchmarks are due almost entirely to the 2-body energies.

We conclude from these comparisons that DMC gives better (in most cases, much better) agreement with the benchmarks than any of the DFT approximations we have studied, with DMC errors being typically five times smaller than those of DFT.

### 3.2.2 A thermal sample of dimer configurations

The thermal sample was produced by drawing 198 configurations at random from the AMOEBA simulation, with O-O distances included out to  $7.5 \text{ \AA}$  but with a bias towards shorter distances. To construct the CCSD(T) benchmark energies for this set, we followed the procedure outlined above for the stationary points. The benchmark energy is computed as

$$E = E^{(1)}(\text{PS}) + E^{(2)}(\text{MP2-F12/AVQZ}) + E^{(2)}(\Delta\text{CCSD(T)-F12/AVTZ}).$$

Because the configuration sample is reasonably large, we are able to analyse the statistics of basis-set differences for the three components. It turns out that the differences depend rather uniformly on  $R_{\text{OO}}$ , providing a simple scheme for partially correcting residual basis-set errors in the MP2-F12 and  $\Delta\text{CCSD(T)-F12}$  correlation contributions. Tests indicate that our benchmark dimer energies are within  $\sim 20 \mu E_h$  of the CBS limit of CCSD(T).

The DMC calculations were performed in the same way as for the stationary points, with the single-electron orbitals and Jastrow factor constructed as described in Sec. 2 and the time-step chosen as before to have the value 0.005 a.u. For every configuration, the DMC run was continued long enough to reduce the statistical error on the total energy to  $60 \mu E_h$ . To characterise the performance of DMC, we show in Fig. 2 the energy difference DMC-bench plotted as a function of  $R_{\text{OO}}$ . The differences are typically on the order of  $100 \mu E_h$ , and there is no obvious dependence of their magnitude on  $R_{\text{OO}}$ . Quantitatively, the mean value of  $E(\text{DMC}) - E(\text{bench})$  over the 198-configuration sample is  $20 \mu E_h$  and the rms fluctuation is  $0.10 mE_h$ . Since the statistical errors of the Monte Carlo sampling in our DMC calculations are  $\sim 60 \mu E_h$ , this means that there are statistically significant deviations of the DMC energies from the CCSD(T) benchmarks, but they appear to be no more than  $\sim 0.1 mE_h$

(2.7 meV).

Our DFT calculations on the thermal sample were done both as direct calculations of the total energy using AV5Z basis set, and also by separating the total energy into 1- and 2-body parts, using the AV5Z basis for  $E^{(1)}$  and AVQZ with counterpoise for  $E^{(2)}$ . A comparison of the direct total energies calculated using AVQZ and AV5Z basis sets shows mean and rms differences of the energies that are less than  $25 \mu E_h$  for all the functionals. The total energies obtained in the direct calculations differ from those obtained by adding the 1- and 2-body energies by at most  $50 \mu E_h$ . The differences  $E(\text{DFT}) - E(\text{bench})$  for the dimer total energies are plotted against  $R_{\text{OO}}$  in Fig. 2. It is immediately clear that the DFT errors are considerably greater than those of DMC, with BLYP and PBE being much inferior to B3LYP and PBE0. The mean values of the DFT-bench differences and their rms fluctuations about these means are reported in Table 3.

An important theme of the present work is the separation of the energy into its many-body parts. We have already seen that some of the DFT approximations suffer from large 1-body errors, so it is natural to ask how they perform when these errors are corrected. If we separate the total energy  $E(\text{DFT})$  computed with a given DFT into its 1-body and 2-body parts, and we then replace the 1-body energy by its Partridge-Schwenke value  $E^{(1)}(\text{PS})$ , we obtain an approximation denoted here by  $\text{DFT}-\Delta_1$ . Clearly, for dimers the errors of  $\text{DFT}-\Delta_1$  are entirely 2-body errors. In Fig. 3, we compare the total-energy differences  $E(\text{DFT}-\Delta_1) - E(\text{bench})$  as a function of  $R_{\text{OO}}$  with the differences  $E(\text{DMC}) - E(\text{bench})$ . The mean and rms values of these differences are reported in Table 3. We see that BLYP is very poor indeed, being much too repulsive over the whole range  $2.5 - 4.5 \text{ \AA}$ , and B3LYP suffers from the same problem, though its errors are smaller. The PBE0 approximation is much better, though it still too repulsive. Best of all these DFTs is PBE. The DMC errors are even small than those of PBE.

These findings are generally in line with what is known from previous DFT and DMC work on the binding energy of the dimer. It is well known that BLYP seriously underbinds, that B3LYP underbinds somewhat less, and that PBE0 and PBE give good binding energies, with PBE being almost exactly correct. It is also known that DMC gives a rather accurate value of the dimer binding energy [60]. The present results enlarge the picture by showing that these errors in the binding energy at the global minimum can be seen as part of general trends over a range of O-O distances.

### 3.3 The trimer

The trimer is important, because it is the smallest cluster for which we can probe beyond-2-body interactions. We created a thermal sample of trimer configurations using the same AMOEBA simulation of liquid water as before, drawing 50 trimer geometries at random, with the condition that all three O-O distances must be less than  $4.5 \text{ \AA}$ .

Our method for obtaining basis-set converged CCSD(T) energies is a straightforward extension of what we

outline above for the dimer. The total trimer energy is decomposed as

$$E = E^{(1)} + E^{(2)} + E^{(3)}(\text{MP2-F12/AVQZ}) + E^{(3)}(\Delta\text{CCSD(T)-F12/AVTZ})$$

where the terms  $E^{(1)} + E^{(2)}$  are treated exactly as in Eq. 4. We find that the Hartree-Fock component  $E^{(3)}(\text{HF})$  converges very rapidly with basis set: the mean difference and the rms fluctuation for AVQZ – AVTZ are only 1.0 and 1.1  $\mu E_h$ . The same is true for the correlation part of  $E^{(3)}(\text{MP2-F12})$ , for which the corresponding values are 1.0 and 1.6  $\mu E_h$ . For  $E^{(3)}(\Delta\text{CCSD(T)-F12})$ , we have results only for AVTZ. However, our calculations on the dimer samples showed that the AVQZ – AVTZ difference for CCSD(T)-F12 was very similar to that of MP2-F12, and we assume the same to be true for  $E^{(3)}$ . From the evidence we have obtained, the energy expression in Eq. 5 should be well within 50  $\mu E_h$  of CCSD(T)/CBS.

Our DMC calculations on the 50-configuration trimer sample follow exactly the methods outlined in Sec. 2. The duration of the DMC runs was long enough to reduce the statistical error on the total energy to 77  $\mu E_h$ . We show in Fig. 4 the errors  $E(\text{DMC}) - E(\text{bench})$  of the DMC total energy of the trimers plotted against the benchmark total energy. We see that the errors and their fluctuations are very small, their mean value and rms fluctuation over the 50-configuration set being 0.30  $mE_h$  (8.1 meV) and 0.13  $mE_h$  (3.5 meV). (Note that these values refer to the *total* energy, not the energy per monomer.)

DFT calculations of the total trimer energy are straightforward, and our tests indicate that the total energy relative to that of three monomers in the PS reference geometry is converged to within 0.15  $mE_h$  with AVQZ basis sets. It is useful to have the many-body decomposition, and we use

$$E(\text{DFT}) = E^{(1)}(\text{DFT/AV5Z}) + E^{(2)}(\text{DFT/AVQZ}) + E^{(3)}(\text{DFT/AVTZ}),$$

again with full counterpoise correction. The two ways of calculating the total trimer energies agree to within mean and rms differences of 120 and 56  $\mu E_h$  respectively. As we show in Fig. 4, the errors of the DFT total energy with PBE, BLYP, B3LYP and PBE0 are much greater than those of DMC: the mean and rms deviations (Table 4) are typically five times greater than the DMC values.

It is now interesting to analyse how much of the DFT errors come from 1-, 2- and 3-body parts of the energy. Here we follow the approach of Taylor *et al.* [100], correcting the low-order many-body contributions to DFT. For example, the effect of 1-body errors can be eliminated by using the energy expression

$$\begin{aligned} E(\text{DFT}-\Delta_1) &= E(\text{DFT}) + E^{(1)}(\text{bench}) - E^{(1)}(\text{DFT}) \\ &\equiv E^{(1)}(\text{bench}) + E^{(2)}(\text{DFT}) + E^{(3)}(\text{DFT}). \end{aligned}$$

The mean and rms deviations  $E(\text{DFT}-\Delta_1) - E(\text{bench}) = [E^{(2)}(\text{DFT}) - E^{(2)}(\text{bench})] + [E^{(3)}(\text{DFT}) - E^{(3)}(\text{bench})]$  are reported in Table 4. As expected from the results of Sec. 3.1, the rms fluctuations of  $E(\text{DFT}-\Delta_1) - E(\text{bench})$  are very much reduced for PBE and BLYP, because their 1-body energies are poor; the mean value of the deviation is improved for PBE but worsened for BLYP, again as expected. On the other hand for B3LYP and particularly for PBE0, correction of the 1-body errors makes little difference.

We can go further by correcting both the 1-body and the 2-body DFT energies, thus obtaining a scheme that we denote by DFT- $\Delta_{12}$ . The trimer energy in this scheme is  $E(\text{DFT-}\Delta_{12}) = E(\text{DFT-}\Delta_1) + [E^{(2)}(\text{bench}) - E^{(2)}(\text{DFT})]$ , which is the same as  $E^{(1)}(\text{bench}) + E^{(2)}(\text{bench}) + E^{(3)}(\text{DFT})$ . The deviations  $E(\text{DFT-}\Delta_{12}) - E(\text{bench}) = E^{(3)}(\text{DFT}) - E^{(3)}(\text{bench})$  now come entirely from DFT errors in the 3-body part. The mean and rms values of these deviations are reported in Table 4. Not surprisingly, these values are very small, so that 3-body effects are quite well represented by all the DFT approximations.

It is clear that the trimer is really too small to yield very interesting conclusions about the accuracy of DFT compared with DMC for beyond-2-body interactions, because there is only a single 3-body term in the total energy. However, as we go to larger clusters, the number of beyond-2-body interactions increases rapidly, so that more interesting comparisons can be made. We therefore turn next to benchmark, DMC and DFT calculations on the tetramer, pentamer and hexamer.

### 3.4 Thermal samples of the tetramer, pentamer and hexamer

Our procedures for the tetramer, pentamer and hexamer follow quite closely those outlined above for the smaller clusters. To generate the samples for cluster size  $N \geq 4$ , we repeatedly planted a sphere of chosen radius  $R(N)$  at a random position at random time-steps of the AMOEBA simulations, and if the number of molecules inside the sphere was equal to  $N$  we accepted these molecules as a sample configuration. (For this purpose, a molecule was counted as being inside the sphere if the O position was inside the sphere.) In making the sample of configurations for a given  $N$ , we chose  $R(N)$  so that the mean number of molecules found inside the sphere was close to  $N$ . In this way, we formed samples of 25 configurations each for  $N = 4, 5$  and 6.

Our benchmark energies were computed as

$$\begin{aligned} E &= E^{(1)}(\text{PS}) + E^{(2)}(\text{MP2-F12/AV5Z}) + E^{(2)}(\Delta\text{CCSD(T)-F12/AVTZ}) \\ &+ E^{(3)}(\text{MP2-F12/AVTZ}) + E^{(3)}(\Delta\text{CCSD(T)-F12/AVDZ}) \\ &+ E^{(>3)}(\text{MP2-F12/AVDZ}) \end{aligned}$$

for the tetramer and pentamer, but for the hexamer we use  $E^{(2)}(\text{MP2-F12/AVQZ})$  in place of  $E^{(2)}(\text{MP2-F12/AV5Z})$ . Contributions up to 3-body were treated using the counterpoise correction as described above; higher-order terms were computed using full counterpoise for the entire cluster; for example, in computing 4-, 5- and 6-body terms for the hexamer, we used the full basis set of the entire cluster for every contribution.

The DMC calculations for the 25-configuration samples of the tetramer, pentamer and hexamer followed exactly the same procedures as before, and the runs were continued until the statistical errors on the total energy were reduced to 0.13, 0.14 and 0.17  $mE_h$  for the tetramer, pentamer and hexamer respectively. As an example of the very close agreement between DMC and the CCSD(T) benchmarks, we show in Fig. 5 the total-energy difference DMC-benchmark for the pentamer configurations plotted against the total energy itself. The

mean value and the rms fluctuations of this difference are reported for all the clusters in Table 4. We see from this that the DMC errors are on the same scale of  $\sim 0.2 mE_h/\text{monomer}$  or less that characterise the recently reported DMC values of the absolute and relative energies of various ice structures [23].

The DFT energies of the  $N \geq 4$  cluster configurations were all computed as sums of many-body contributions. For the 1-, 2- and 3-body energies, we employed AV5Z, AVQZ and AVTZ basis sets respectively, with full counterpoise for all dimers and trimers for the 2- and 3-body energies. In the ( $n \geq 4$ )-body parts, we found it more convenient to use full counterpoise for the entire cluster, as we did for the CCSD(T) benchmarks, and for this purpose we used AVDZ basis sets. To cross-check the total energies obtained in this way, we also computed them directly (i.e. without many-body decomposition), using AVQZ basis sets.

As an example of DFT performance, we show in Fig. 5 the differences DFT-benchmark for the pentamer sample plotted against the benchmark total energies. The mean values of these differences and their rms fluctuations are reported for all the larger clusters in Table 4. It is evident that the accuracy of DMC is very much greater than any of the DFT approximations. As might be expected from our results for the smaller clusters, BLYP is very poor, having rms deviations from the benchmarks that are about 10 times the size of those with DMC, and its mean deviations are also large. For all the clusters, PBE is somewhat better and B3LYP still better, but best of all is PBE0, whose rms errors are a little over 2.5 times those of DMC.

In our discussion of DFT errors for the trimer (Sec. 3.3), we pointed out the possibility of correcting DFT first for 1-body errors and then for both 1-body and 2-body errors, these two levels of corrected DFT being denoted by DFT- $\Delta_1$  and DFT- $\Delta_{12}$ . Since we have all the  $n$ -body parts of both benchmark and DFT energies of the tetramer, pentamer and hexamer, we can make the same analysis for them. We report in Table 4 the mean and rms deviations of the DFT- $\Delta_1$  and DFT- $\Delta_{12}$  energies away from the benchmarks. As expected, correction of the 1-body energy substantially reduces the rms errors of PBE and BLYP, because these DFTs have quite large 1-body errors, but it makes rather little difference in the case of B3LYP and PBE0, because their 1-body errors are small. Interestingly, this correction considerably worsens the mean BLYP errors, because in the uncorrected version there is a partial cancellation of errors between the 1- and 2-body parts. Correcting for both 1- and 2-body errors, the approximations suffer only from ( $n \geq 3$ )-body errors, which we also report in Table 4. Clearly, these errors are extremely small. Indeed, the corrected DFTs B3LYP- $\Delta_{12}$  and PBE0- $\Delta_{12}$  are even slightly better than DMC.

The comparisons we have presented demonstrate the high accuracy of DMC, but they also indicate that the 1-body, 2-body and beyond-2-body parts of the total energy are individually well described by DMC. However, there is another aspect of DMC predictions that is worth examining. If we judged solely by our comparisons for the thermal samples, we would infer that all the main errors of DFT are in the 1- and 2-body parts, so that once these are corrected we get approximations that are as good as DMC. However, this inference is not true in general, as we will show next by a many-body analysis of the stable isomers of the hexamer.

### 3.5 Stable isomers of the hexamer

The global- and local-minimum structures of the H<sub>2</sub>O hexamer have long played a role in the understanding of water energetics, because their relative energies are determined by a rather delicate interplay between different kinds of interactions [35, 36, 61, 37, 49, 101, 102, 103]. The isomers we will be concerned with here are the prism, cage, book and ring, whose geometries have been presented in many previous papers (see e.g. Ref. [61]). The atomic coordinates that we use here are the MP2/AVTZ-optimised structures of Santra *et al.* [61]. The more open structures, such as the ring, favour hydrogen bonding with OH $\cdots$ O angles that maximise the strengths of individual hydrogen bonds. In the more compact structures, including the prism and cage, the total number of hydrogen bonds is greater, but the OH $\cdots$ O angles are less favourable. The book structure is a compromise between the two kinds. Coupled-cluster CCSD(T) calculations near the basis-set limit leave no doubt that the more compact structures are more stable, the consensus being that the prism is the global minimum, with the cage slightly above it [37]. The ring is less stable by  $\sim 3.0 mE_h$  in the total energy, and the book has an intermediate energy. DMC calculations give the correct energy ordering and energy differences that agree closely with the CCSD(T) values [61], and we noted in the Introduction that this is one of the key pieces of evidence for the accuracy of DMC. Most of the conventional DFT approximations give the wrong energy ordering, with BLYP and B3LYP making the ring the global minimum, and PBE giving this honour to the book [36]. The reasons for this have been widely discussed, and a many-body analysis has already been used to identify the cause of the problems, the suggestion being that the lack of long-range dispersion is responsible [61]. A detailed break-down of the contributions to the relative energies of isomers of the hexamer has also been reported by Wang *et al.* [104]. We find it worthwhile to revisit this question, because DMC can now be compared with more accurate CCSD(T) results than were available before and because our own many-body analysis indicates that the lack of dispersion may not be the only cause of DFT errors.

We report in Table 5 our MP2 and CCSD(T) results for the prism, cage, book and ring isomers, computed in all cases with the MP2-optimized structures given by Santra *et al.* [61], which are also the structures used in their DMC calculations. Our MP2 energies come from direct calculations on the entire hexamer, using AVQZ basis sets with F12. The CCSD(T) energies reported in the Table, do not, however, come from direct calculations on the cluster; instead, we compute

$$E = E(\text{MP2-F12/AVQZ}) + \sum_{i=1}^3 E^{(i)}(\Delta\text{CCSD(T)-F12})$$

As shown in the Table, our MP2 energy differences between the isomers agree very closely with earlier highly converged results, and our CCSD(T) energy differences also agree very well with recent CCSD(T) results close to the CBS limit. In agreement with previous work, we find that on going from MP2 to CCSD(T) the energy difference between the prism and the cage increases significantly, and the energy of the ring above the prism increases by  $\sim 1.0 mE_h$ . The Table also gives the DMC energy differences of Santra *et al.*, and we note that they agree very closely with the CCSD(T) results reported here. Importantly, DMC is closer to the CCSD(T)

energies than to those from MP2. Our own PBE, BLYP, B3LYP and PBE0 energies computed with AV5Z basis sets are also included in the Table. We fully confirm the conclusions from previous work that these DFTs give completely erroneous trends, wrongly predicting that the less compact isomers are more stable than the compact ones. The quantitative errors of the DFT energy differences are substantial, with the energy difference between the ring and the prism being in error by as much as  $5 mE_h$  in some cases.

To understand the origin of the erroneous DFT predictions, we compare in Fig. 6 the 2-body and 3-body energies from benchmark CCSD(T) and from DFT. The 2-body benchmark energies were obtained using MP2-F12/AVQZ and  $\Delta$ CCSD(T)-F12/AVTZ, while for the 3-body benchmarks we used AVTZ for all parts. The DFT 2- and 3-body energies were computed using AVQZ and AVTZ respectively. It is clear from the 2-body results that BLYP and B3LYP predict much too weak a lowering of 2-body energy as we go from the ring to the cage and prism, while PBE is rather accurate and PBE0 is less accurate than PBE but better than BLYP and B3LYP. (The difference of 2-body energies of ring and prism is  $10.0 mE_h$  according to CCSD(T), but is only  $3.4$  and  $4.7 mE_h$  with BLYP and B3LYP respectively, so that BLYP is in error by a factor of 3 and B3LYP by a factor of 2.) This is what we should expect from the 2-body energies presented in Sec. 3.2.2, since BLYP and B3LYP are systematically too repulsive over a rather wide range of distances, while the errors of PBE and PBE0 are much smaller. By contrast, in the 3-body energy the situation is reversed, with B3LYP now being almost perfect and BLYP only a little worse, while PBE and PBE0 are both rather poor. (The ring-prism difference of 3-body energy is  $5.01 mE_h$  according to CCSD(T), but PBE and PBE0 give  $8.38$  and  $6.97 mE_h$  respectively.) We expect from this that if we correct the DFT approximations for their 1- and 2-body errors, thus obtaining what we referred to earlier as DFT- $\Delta_{12}$ , then BLYP- $\Delta_{12}$  and B3LYP- $\Delta_{12}$  should agree rather well with CCSD(T) and DMC, while PBE- $\Delta_{12}$  and PBE0- $\Delta_{12}$  should be less good. This expectation is confirmed by our DFT- $\Delta_{12}$  energies reported in Table 5. If we now correct also for 3-body errors, we would expect this to give little further improvement for BLYP and B3LYP, but substantial improvements for PBE and PBE0, and the DFT- $\Delta_{123}$  results of Table 5 confirm this.

These comparisons are very useful for our assessment of the accuracy of DMC, because they indicate that DMC must be accurate not only for the 2-body energy, as we already know from Sec. 3.2, but also for the 3-body energy. We can draw this conclusion because PBE and DMC have very similar, and very small errors for 2-body energy, but DMC is very much better than PBE for the hexamer isomers, and we have traced the main cause of this to the 3-body energy.

## 4 Discussion and conclusions

The main aims of the present work have been to assess the accuracy of diffusion Monte Carlo (DMC) for water clusters by comparing with quantum chemistry benchmarks, and to investigate how well it overcomes the deficiencies of common DFT approximations. We noted in the Introduction that any method that is intended

to give an accurate description of cluster and bulk water and ice systems across a wide range of conditions must be accurate for all the key components of the energy, including the distortion energy of the H<sub>2</sub>O monomer, the 2-body interactions that determine the energetics of the water dimer, and the many-body contributions arising from polarisability and other mechanisms that are known to be crucial for larger clusters and for the bulk liquid and solid phases. Our comparisons with well converged CCSD(T) energies for both statistical samples of configurations and in some cases for sets of stable isomers show that DMC gives all the main components of the energy rather accurately, while the standard DFT approximations that we have studied encounter problems with one or more of these components. We have emphasised the importance of studying random thermal samples, since these allow us to characterise the accuracy of QMC and DFT approximations across an entire domain of configurations, rather than at a small number of special configurations. At the same time, we have noted that the mean and rms errors of any given approximation will depend on the choice of thermal sample.

The importance of achieving an accurate description of monomer energetics was emphasised in a recent paper of Santra *et al.* [64], who showed that some commonly used DFT functionals give a rather poor description of the distortion energy, making bond-stretching too easy. We have confirmed this on a thermal sample of 100 distorted monomer configurations drawn from a classical m.d. simulation of liquid water performed with the flexible AMOEBA interaction model. We found poor accuracy with PBE and BLYP, better accuracy with B3LYP and excellent accuracy with PBE0, in agreement with Ref. [64]. The accuracy of DMC turns out to be even better than PBE0. It has been suggested that the excessive deformability of the H<sub>2</sub>O monomer with PBE and BLYP may be a significant factor in their rather poor predictions for bulk water. The very high accuracy of DMC for the monomer means that it does not suffer from such problems.

Our calculations on the 10 stationary points of the H<sub>2</sub>O dimer provide important evidence that the accuracy of DMC for the 2-body energy of water systems is also very good. All the energies come in the correct order, though we recall that this is also achieved by most DFT approximations. Much more significant is the very close agreement with highly converged CCSD(T) benchmarks for the energies relative to the global minimum, which are almost all reproduced by DMC to within  $0.1 mE_h$  (2.7 meV). By contrast, DFT errors for the relative energies are typically  $0.5 - 1.0 mE_h$ , and no DFT approximation that we are aware of comes near the accuracy of DMC. We note that these comparisons give a direct test of the 2-body energy, since the monomer distortion energies at the 10 stationary points are extremely small.

More relevant to bulk-phase water are our comparisons between DMC, DFT and CCSD(T) benchmarks for a large random thermal sample of dimer configurations drawn from the AMOEBA m.d. simulation of bulk water. This sample is large enough for us to examine errors as a function of O-O distance, and we have seen that DMC reproduces the benchmarks accurately and consistently throughout the range  $2.5 - 7.0 \text{ \AA}$  that we have examined. The DMC errors barely exceed the statistical errors of the Monte Carlo sample of the DMC calculations themselves, the mean and rms deviation of the DMC energy from the CCSD(T) benchmarks being



0.018 and 0.102  $mE_h$  (0.5 and 2.8 meV). These errors are of about the size that might be expected from previous DMC work on the  $H_2O$  dimer. On the other hand, the errors of the total dimer energy with all the DFT approximations examined here are very much greater (see Table 3). However, in the case of PBE and BLYP, the errors in the monomer distortion energy contribute significantly. In practical calculations using these approximations on clusters or bulk systems, it would be perfectly straightforward to correct for these 1-body errors, simply by adding the difference between the essentially exact Partridge-Schwenke and the DFT distortion energies. If we do this for our dimer samples, then we obtain corrected DFT approximations which we refer to as DFT- $\Delta_1$ , whose errors are solely in the 2-body part. We have seen that the 2-body energy of BLYP is much too repulsive and B3LYP suffers from the same problem, as would be expected from the substantial underbinding of the dimer with BLYP and B3LYP. However, for PBE, the 2-body energy turns out to be very good, its quality being comparable with that of DMC, so that if we simulated the dimer with PBE corrected for 1-body errors, rather accurate results would be obtained; the approximation PBE0- $\Delta_1$  is also quite respectable.

For the larger clusters from the trimer to the hexamer, we have followed a similar procedure, drawing sets of configurations at random from the AMOEBA m.d. simulation and comparing DMC, DFT and benchmark CCSD(T) energies for these samples, taking care as usual that the total energies with DFT and CCSD(T) are basis-set converged to  $\sim 0.1 mE_h$  or better. For these clusters, the thermal samples are smaller than for the dimer, consisting of 50 configurations for the trimer and 25 each for the tetramer, pentamer and hexamer. Since the errors in either or both of the 1-body and 2-body components with the DFT approximations are considerably larger than those of DMC, we expect that DMC will substantially outperform them for these large clusters, and this is indeed what we find. However, this is not the whole story, because it is possible that some of the problems encountered by DFT approximations in treating bulk liquid water and ice may be associated with many-body (i.e. beyond-2-body) components of the energy, perhaps because their description of the relevant polarisabilities is inadequate. We have therefore tried to test whether DMC also outperforms DFT for these many-body contributions.

One way we have used to test the quality of the DMC beyond-2-body energy is based on making a many-body decomposition of the DFT total energy for our thermal samples of the trimer and higher clusters, and then to replace the DFT 1- and 2-body energies by the benchmark energies (i.e. Partridge-Schwenke for 1-body and near-CBS CCSD(T) for 2-body). Any remaining errors in the resulting corrected versions of DFT, which we refer to as DFT- $\Delta_{12}$ , are then due entirely to errors in the beyond-2-body energy. If we then compare with DMC, we are putting DMC to an extreme and certainly unfair test, since it has to compete unaided against massively assisted DFT. Remarkably, DMC survives even this rather well, having errors in its total energy that are still smaller than or comparable with the errors in the beyond-2-body energy for the DFT approximations.

We have noted that the relative energies of the well-known isomers of the  $H_2O$  hexamer also provide an excellent way of testing the beyond-2-body energy of DMC. The point here is that all the DFT approximations

we examined give completely erroneous energy orderings of these isomers. It has been shown in earlier work [61] that DMC gives the energy differences between these isomers in excellent agreement with CCSD(T), and we confirmed this here by comparing with the improved CCSD(T) energies now available. As also pointed out earlier, a many-body decomposition of the DFT and CCSD(T) energies allows one to determine where the DFT errors come from. We have presented our own many-body analysis showing that for some of the DFTs (e.g. BLYP) the errors lie mainly in the 2-body part, whereas in others (e.g. PBE) the 2-body component is accurate, but there are substantial errors in the beyond-2-body components. Since we know that DMC gives an accurate account of the 2-body component, these comparisons confirm its accuracy also for the beyond-2-body components.

It is intriguing that the isomers of the hexamer reveal the superiority of DMC over some of the DFTs for beyond-2-body energy in a much clearer way than the thermal sample of hexamer configurations. The implication of this is that thermal samples of cluster configurations drawn from a realistic model of the liquid do not necessarily suffice for a full assessment of the errors of approximate methods. It is instructive to note that if an isolated hexamer in free space were simulated in thermal equilibrium using one of our DFT approximations, a completely erroneous distribution consisting mainly of ring-like structures would be observed, whereas if the simulation were performed with DMC (assuming this to be feasible), a much more realistic distribution consisting mainly of compact structures would be observed. However, the thermal sample of configurations generated by DMC would not suffice to assess fully the errors of DFT, because these errors only become apparent for thermal samples that include both open and compact structures. Similarly in assessing DFT errors using thermal samples relevant to the liquid, it seems desirable to use a wider range of configurations than those that occur commonly in the real liquid. This is an important matter for future study.

The present comparative study on water clusters, taken together with the recently demonstrated high accuracy of DMC for the energetics of several ice crystal structures [23], indicates that DMC has the accuracy needed to serve as a benchmarking tool for water systems across a wide range of conditions. Its advantages over correlated quantum chemistry techniques are that its scaling with system size is much more favourable, convergence to the basis-set limit is easily achieved, it is straightforward to apply to periodic systems, and its parallel scaling on large supercomputers is essentially perfect. In the immediate future, we plan to use DMC to obtain benchmark energies for thermal samples of much larger water clusters than those studied here. These benchmarks will then be used to test DFT approximations. We expect to find ways of separating both the benchmark and the DFT total energies into their 1-, 2- and beyond-2-body contributions, as we have done here, so that we can analyse the origin of DFT errors. It should also be possible to do the same for bulk water itself. As we noted in the Introduction, DMC calculations on thermal samples of periodic liquid water configurations were already demonstrated some years ago [80], so that the technical feasibility of what we suggest is not in doubt. The possibility of tuning DFT approximations to reproduce DMC and quantum chemistry benchmarks

for a range of water systems is also an interesting possibility for the future. It is worth adding that tests of DMC against CCSD(T) for larger clusters should be possible in the future, because the availability of quantum chemistry codes that can be run on very large parallel computers is already making it possible to perform coupled-cluster calculations on much larger molecular systems than before [38].

In conclusion, we have shown that the accuracy of DMC for thermal and other configuration samples of H<sub>2</sub>O clusters from the monomer to the hexamer is excellent, the errors of DMC being typically 0.1 – 0.2 mE<sub>h</sub> (2.5 – 5.0 meV) per molecule. This error is much smaller than the typical DFT errors, and this, together with other evidence for the accuracy of DMC, supports its reliability as a source of benchmarks for testing and calibrating DFT. It is desirable to extend the tests of DMC accuracy to larger clusters, and we have indicated how this might be possible. We have also suggested how DMC calculations can be used to improve the understanding of both liquid and solid bulk water.

## Acknowledgments

The work of MDT is supported by EPSRC grant EP/I030131/1, and that of FRM by EPSRC grant EP/F000219/1. DMC calculations were performed on the Oak Ridge Leadership Computing Facility, located in the National Center for Computational Sciences at Oak Ridge National Laboratory, which is supported by the Office of Science of the Department of Energy under contract DE-AC05-00OR22725 (USA).

## References

- [1] K. Laasonen, M. Sprik, M. Parrinello and R. Car, *J. Chem. Phys.*, **99**, 9080 (1993).
- [2] M. E. Tuckerman, K. Laasonen, M. Sprik and M. Parrinello, *J. Chem. Phys.*, **103**, 150 (1995).
- [3] M. Sprik, J. Hutter and M. Parrinello, *J. Chem. Phys.*, **105**, 1142 (1996).
- [4] P. L. Silvestrelli and M. Parrinello, *J. Chem. Phys.*, **111**, 3572 (1999).
- [5] C. Lee, D. Vanderbilt, K. Laasonen, R. Car and M. Parrinello, *Phys. Rev. Lett.*, **69**, 462 (1992).
- [6] D. R. Hamann, *Phys. Rev. B*, **55**, R10157 (1997).
- [7] S. J. Singer, J.-L. Kuo, T. K. Hirsch, C. Knight, L. Omajäe and M. L. Klein, *Phys. Rev. Lett.*, **94**, 135701 (2005).
- [8] M. de Koning, A. Antonelli, A. J. R. da Silva and A. Fazio, *Phys. Rev. Lett.*, **96**, 075501 (2006).
- [9] I.-F. W. Kuo and C. J. Mundy, *Science*, **303**, 658 (2004).
- [10] D. Pan, L.-M. Liu, G. A. Tribello, B. Slater, A. Michaelides and E. Wang, *Phys. Rev. Lett.*, **101**, 155703 (2008).
- [11] D. Marx, M. Sprik and M. Parrinello, *Chem. Phys. Lett.*, **273**, 360 (1997).
- [12] Y. Tateyama, J. Blumberger, M. Sprik and I. Tavernelli, *J. Chem. Phys.*, **122**, 234505 (2005).
- [13] L.-M. Liu, M. Krack and A. Michaelides, *J. Chem. Phys.*, **130**, 234702 (2009).
- [14] L.-M. Liu, C. Zhang, G. Thornton and A. Michaelides, *Phys. Rev. B*, **82**, 161415(R), (2010).
- [15] J. C. Grossman, E. Schwegler, E. W. Draeger, F. Gygi and G. Galli, *J. Chem. Phys.*, **120**, 300 (2004).
- [16] M. Allesch, E. Schwegler, F. Gygi and G. Galli, *J. Chem. Phys.*, **120**, 5192 (2004).
- [17] M. V. Fernández-Serra and E. Artacho, *J. Chem. Phys.*, **121**, 11136 (2004).
- [18] J. VandeVondele, F. Mohamed, M. Krack, J. Hutter, M. Sprik and M. Parrinello, *J. Chem. Phys.*, **122**, 014515 (2005).
- [19] H.-S. Lee and M. E. Tuckerman, *J. Chem. Phys.*, **125**, 154507 (2006).
- [20] T. Todorova, A. P. Seitsonen, J. Hutter, I.-F. W. Kuo and C. J. Mundy, *J. Phys. Chem. B*, **110**, 3685 (2006).
- [21] M. Guidon, F. Schiffmann, J. Hutter and J. VandeVondele, *J. Chem. Phys.*, **128**, 214104 (2008).
- [22] J. Wang, G. Román-Pérez, J. M. Soler, E. Artacho and M. V. Fernández-Serra, *J. Chem. Phys.*, **134**, 024516 (2011).
- [23] B. Santra, J. Klimeš, D. Alfè, A. Tkatchenko, B. Slater, A. Michaelides, R. Car and M. Scheffler, *Phys. Rev. Lett.*, **107**, 185701 (2011).

- [24] A. Møgelhøj, A. K. Kelkkanen, K. T. Wikfeldt, J. Schiøtz, J. J. Mortensen, L. G. M. Pettersson, B. I. Lundqvist, K. W. Jacobsen, A. Nilsson and J. K. Nørskov, *J. Phys. Chem. B*, **115**, 14149 (2011).
- [25] S. S. Xantheas, *J. Chem. Phys.*, **100**, 7523 (1994).
- [26] S. S. Xantheas, *J. Chem. Phys.*, **102**, 4505 (1995).
- [27] J. M. Pedulla, F. Vila and K. D. Jordan, *J. Chem. Phys.*, **105**, 11091 (1996).
- [28] C. J. Burnham, J. Li, S. S. Xantheas and M. Leslie, *J. Chem. Phys.*, **110**, 4566 (1999).
- [29] C. J. Burnham and S. S. Xantheas, *J. Chem. Phys.*, **116**, 1500 (2002).
- [30] W. Klopper, J. G. C. M. van Duijneveldt-van de Rijdt and R. B. van Duijneveldt, *Phys. Chem. Chem. Phys.*, **2**, 2227 (2000).
- [31] G. S. Tschumper, M. L. Leininger, B. C. Hoffman, E. E. Valeev, H. F. Schaeffer and M. Quack, *J. Chem. Phys.*, **116**, 690 (2002).
- [32] X. Xu and W. A. Goddard III, *J. Phys. Chem. A*, **108**, 2305 (2004).
- [33] Y. Zhao and D. G. Truhlar, *J. Chem. Theory Comput.*, **1**, 415 (2005).
- [34] J. A. Anderson and G. S. Tschumper, *J. Phys. Chem. A*, **110**, 7268 (2006).
- [35] R. M. Olson, J. L. Bentz, R. A. Kendall, M. W. Schmidt and M. S. Gordon, *J. Chem. Theory Comput.*, **3**, 1312 (2007).
- [36] E. E. Dahlke, R. M. Olson, H. R. Leverentz and D. G. Truhlar, *J. Phys. Chem. A*, **112**, 3976 (2008).
- [37] D. M. Bates and G. S. Tschumper, *J. Phys. Chem. A*, **113**, 3555 (2009).
- [38] S. Yoo, E. Aprà, X. C. Zeng and S. S. Xantheas, *J. Phys. Chem. Lett.*, **1**, 3122 (2010).
- [39] H. Popkie, H. Kistenmacher and E. Clementi, *J. Chem. Phys.*, **59**, 1325 (1973).
- [40] O. Matsuoka, E. Clementi and M. Yoshimine, *J. Chem. Phys.*, **64**, 1351 (1976).
- [41] K. Kim and K. D. Jordan, *J. Phys. Chem.*, **98**, 10089 (1994).
- [42] M. P. Hodges, A. J. Stone and S. S. Xantheas, *J. Phys. Chem. A*, **101**, 9163 (1997).
- [43] E. M. Mas, R. Bukowski and K. Szalewicz, *J. Chem. Phys.*, **118**, 4404 (2003).
- [44] X. Huang, B. J. Braams and J. M. Bowman, *J. Phys. Chem. A*, **110**, 445 (2006).
- [45] R. Bukowski, K. Szalewicz, G. C. Groenenboom and A. van der Avoird, *Science*, **315**, 1249 (2007).
- [46] X. Huang, B. J. Braams, J. M. Bowman, R. E. A. Kelly, J. Tennyson, G. C. Groenenboom and A. van der Avoird, *J. Chem. Phys.*, **128**, 034312 (2008).
- [47] G. S. Fanourgakis and S. S. Xantheas, *J. Chem. Phys.*, **128**, 074506 (2008).
- [48] K. Szalewicz, C. Leforestier and A. van der Avoird, *Chem. Phys. Lett.*, **482**, 1 (2009).

- [49] R. Kumar, F. F. Wang, G. R. Jenness and K. D. Jordan, *J. Chem. Phys.*, **132**, 014309 (2010).
- [50] Y. Wang, X. Huang, B. C. Shepler, B. Braams and J. M. Bowman, *J. Chem. Phys.*, **134**, 094509 (2011).
- [51] A. Erba, S. Casassa, L. Maschio and C. Pisani, *J. Phys. Chem. B*, **113**, 2347 (2009).
- [52] D. P. O'Neill, N. L. Allan and F. R. Manby, in *Accurate Condensed-Phase Quantum Chemistry*, ed. F. R. Manby, CRC Press, Boca Raton (2011), p. 163.
- [53] B. L. W. Hammond, W. A. Lester and P. J. Reynolds, *Monte Carlo Methods in Ab Initio Quantum Chemistry*, World Scientific, Singapore (1994).
- [54] J. B Anderson, *Rev. Comput. Chem.*, **13**, 133 (1999).
- [55] M. P. Nightingale and C. J. Umrigar (eds), *Quantum Monte Carlo Methods in Physics and Chemistry*, Vol. 525 of NATO Advance-Study Institute, Series C: Mathematical and Physical Sciences, Kluwer Academic, Dordrecht (1999).
- [56] W. M. C. Foulkes, L. Mitaš, R. J. Needs and G. Rajagopal, *Rev. Mod. Phys.*, **73**, 33 (2001).
- [57] R. J. Needs, M. D. Towler, N. D. Drummond and P. López-Ríos, *J. Phys. Condens. Matter*, **22**, 023201 (2010).
- [58] M.D. Towler, in 'Computational Methods for Large Systems' (Wiley, 2011), p. 119.
- [59] B.M. Austin, D.Y. Zubarev, and W.A. Lester, Jr., *Chem. Rev.* **112**, 263 (2012)
- [60] I. G. Gurtubay and R. J. Needs, *J. Chem. Phys.*, **127**, 124306 (2007).
- [61] B. Santra, A. Michaelides, M. Fuchs, A. Tkachenko, C. Filippi and M. Scheffler, *J. Chem. Phys.*, **129**, 194111 (2008).
- [62] M. Korth, A. Lüchow and S. Grimme, *J. Phys. Chem. A*, **112**, 2104 (2008).
- [63] J. Ma, D. Alfè, A. Michaelides and E. Wang, *J. Chem. Phys.*, **130**, 154303 (2009).
- [64] B. Santra, A. Michaelides and M. Scheffler, *J. Chem. Phys.*, **131**, 124509 (2009).
- [65] S. Tsuzuki and H. P. Lüthi, *J. Chem. Phys.*, **114**, 3949 (2001).
- [66] D. Hankins, J. W. Moskowitz and F. H. Stillinger, *J. Chem. Phys.*, **53**, 4544 (1970).
- [67] J. C. White and E. R. Davidson, *J. Chem. Phys.*, **93**, 8029 (1990).
- [68] H. Partridge and D. W. Schwenke, *J. Chem. Phys.*, **106**, 4618 (1997).
- [69] J. Ireta, J. Neugebauer and M. Scheffler, *J. Phys. Chem. A*, **108**, 5692 (2004).
- [70] B. Santra, A. Michaelides and M. Scheffler, *J. Chem. Phys.*, **127**, 184104 (2007).
- [71] J. T. Su, X. Xu and W. A. Goddard III, *J. Phys. Chem. A*, **108** 10518 (2004).
- [72] D. M. Ceperley and B. J. Alder, *Phys. Rev. Lett.*, **45**, 566 (1980); P. J. Reynolds, D. M. Ceperley, B. J. Alder and W. A. Lester, *J. Chem. Phys.*, **77**, 5593 (1982).

- [73] L. Mitaš, E. L. Shirley, and D. M. Ceperley, *J. Chem. Phys.*, **95**, 3467 (1991).
- [74] C. J. Umrigar, K. G. Wilson, and J. M. Wilson, *Phys. Rev. Lett.*, **60**, 1719 (1988).
- [75] CASINO 2.8 User Manual, R. J. Needs, M. D. Towler, N. D. Drummond and P. López-Ríos (University of Cambridge, Cambridge, 2010). CASINO web-site: [www.tcm.phy.cam.ac.uk/~mdt26/casino.html](http://www.tcm.phy.cam.ac.uk/~mdt26/casino.html).
- [76] N.D. Drummond, M.D. Towler, and R.J. Needs, *Phys. Rev. B*, **70**, 235119 (2004).
- [77] J. R. Trail and R. J. Needs, *J. Chem. Phys.*, **122**, 014112 (2005); J. R. Trail and R. J. Needs, *J. Chem. Phys.*, **122**, 174109 (2005).
- [78] P. Gianozzi, S. Baroni, N. Bonini, M. Calandra, R. Car, C. Cavazzoni, D. Ceresoli, G. L Chiarotti, M. Cococcioni, I. Dabo, A. Dal Corso, S. Fabris, G. Fratesi, S. de Gironcoli, R. Gebauer, U. Gerstmann, C. Gougouris, A. Kokalj, M. Lazzeri, L. Martin-Samos, N. Marzari, F. Mauri, R. Mazzarello, S. Paolini, A. Pasquarello, L. Paulatto, C. Sbraccia, S. Scandolo, G. Sclauzero, A. P Seitsonen, A. Smogunov, P. Umari and R. M. Wentzcovitch, *J. Phys. Condens. Matter*, **21**, 395502 (2009).
- [79] D. Alfè and M. J. Gillan, *Phys. Rev. B*, **70**, 161101(R) (2004).
- [80] J. C. Grossman and L. Mitaš, *Phys. Rev. Lett.*, **94**, 056403 (2005).
- [81] A. L. East and W. D. Allen, *J. Chem. Phys.*, **99**, 4638 (1993).
- [82] N. L. Allinger, J. T. Fermann, W. D. Allen and H. F. Schaefer III, *J. Chem. Phys.* **106**, 5143 (1997).
- [83] MOLPRO 2009.1, a package of *ab initio* programs, H.-J. Werner, P. J. Knowles, R. Lindh, F. R. Manby, M. Schütz, and others, see <http://www.molpro.net>.
- [84] H.-J. Werner, P. J. Knowles, G. Knizia, F. R. Manby and M. Schütz, *Comput. Mol. Sci.*, in press, DOI: 10.1002/wcms.82 (2011).
- [85] T. H. Dunning, *J. Chem. Phys.*, **90**, 1007 (1989).
- [86] R. A. Kendall, T. H. Dunning, Jr. and R. J. Harrison, *J. Chem. Phys.*, **96**, 6796 (1992).
- [87] W. Kutzelnigg, *Theor. Chim. Acta*, **68**, 445 (1985).
- [88] W. Kutzelnigg and W. Klopper, *J. Chem. Phys.*, **94**, 1985 (1991).
- [89] W. Klopper, F. R. Manby, S. Ten-no and E. F. Valeev, *Int. Rev. Phys. Chem.*, **25**, 427 (2006).
- [90] H.-J. Werner, T. B. Adler and F. R. Manby, *J. Chem. Phys.*, **126**, 164102 (2007).
- [91] T. B. Adler, G. Knizia and H.-J. Werner, *J. Chem. Phys.*, **127**, 221106 (2007).
- [92] F. R. Manby, *J. Chem. Phys.*, **119**, 4607 (2003).
- [93] H.-J. Werner, F. R. Manby and P. J. Knowles, *J. Chem. Phys.*, **118**, 8149 (2003).
- [94] R. Polly, H.-J. Werner, F. R. Manby and P. J. Knowles, *Molec. Phys.*, **102**, 2311 (2004).
- [95] S. F. Boys and F. Bernardi, *Molec. Phys.*, **19**, 553 (1970).

- [96] The benefits of using counterpoise for the water dimer are outlined in T. Helgaker, P. Jørgensen and J. Olsen, *Molecular Electronic-Structure Theory* (Wiley, 2000), Ch. 8.5.
- [97] P. Ren and J. W. Ponder, *J. Phys. Chem. B*, **107**, 5933 (2003).
- [98] P. Ren and J. W. Ponder, *J. Phys. Chem. B*, **108**, 13427 (2004).
- [99] B. J. Smith, D. J. Swanton, J. A. Pople, H. F. Schaefer and L. Radom, *J. Chem. Phys.*, **92**, 1240 (1990).
- [100] C. R. Taylor, P. J. Bygrave, J. N. Hart, N. L. Allan and F. R. Manby, submitted (2012).
- [101] K. Kim, K. D. Jordan and T. S. Zwier, *J. Amer. Chem. Soc.*, **116**, 11568 (1994).
- [102] K. Liu, M. G. Brown, R. J. Saykally, J. K. Gregory and D. C. Clary, *Nature*, **381**, 501 (1996).
- [103] S. S. Xantheas, C. J. Burnham and R. J. Harrison, *J. Chem. Phys.*, **116**, 1493 (2002).
- [104] F.-F. Wang, G. Jenness, W. A. Al-Saidi and K. D. Jordan, *J. Chem. Phys.*, **132**, 134303 (2010).
- [105] S. Yoo, X. C. Zeng and S. S. Xantheas, *J. Chem. Phys.*, **130**, 221102 (2009).



# Tables

	mean	rms
DMC	0.01	0.04
PBE	-0.37	0.54
BLYP	-0.45	0.63
B3LYP	-0.14	0.20
PBE0	-0.01	0.08

Table 1: Mean values and rms fluctuations of DMC and DFT errors of monomer energy for a thermal sample of 100 configurations (see text). The Partridge-Schwenke (PS) energy function is used as the “exact” energy, and the energy zero for DMC and DFT approximations is taken to be the energy in the PS equilibrium geometry. Units:  $mE_h$ .

s.p.	CCSD(T)	DMC	PBE	BLYP	B3LYP	PBE0
1	0.000	0.000	0.000	0.000	0.000	0.000
2	0.783	0.866	0.904	0.838	0.834	0.867
3	0.910	1.001	1.288	1.194	1.040	1.085
4	1.115	1.250	1.707	1.814	1.690	1.627
5	1.519	1.445	2.374	2.406	2.208	2.187
6	1.603	1.505	2.707	2.676	2.382	2.401
7	2.893	2.863	3.544	3.534	3.447	3.395
8	5.663	5.739	5.869	5.698	5.881	5.883
9	2.840	2.910	3.502	3.485	3.371	3.304
10	4.307	4.471	4.838	4.591	4.601	4.654

Table 2: Comparison of DMC energies and DFT energies given by the PBE, BLYP, B3LYP and PBE0 functionals with CCSD(T) benchmarks for the 10 stationary points of the  $H_2O$  dimer. For each set of energies, the zero of energy has been taken so that the energy of the global minimum geometry is equal to zero. Numbering of stationary points follows that of previous authors (see e.g. Refs. [31]). Energy units:  $mE_h$ .

method	mean error	rms error
DMC	0.018	0.102
PBE	-0.681	0.783
BLYP	-0.155	1.102
B3LYP	0.180	0.463
PBE0	0.093	0.177
PBE- $\Delta_1$	0.056	0.144
BLYP- $\Delta_1$	0.736	0.679
B3LYP- $\Delta_1$	0.469	0.371
PBE0- $\Delta_1$	0.111	0.133

Table 3: DMC and DFT mean and rms fluctuation of errors of the total energy for thermal sample of 198 dimer configurations. In the case of DFT, the approximations denoted by PBE- $\Delta_1$  etc represent the total energy after correction for errors of the 1-body energy (see text). Units:  $mE_h$ .

DFT	DFT	DFT- $\Delta_1$	DFT- $\Delta_{12}$
trimer			
PBE	-0.034 (0.376)	0.152 (0.137)	0.062 (0.049)
BLYP	0.517 (0.413)	1.101 (0.256)	-0.023 (0.039)
B3LYP	0.542 (0.175)	0.709 (0.147)	-0.011 (0.028)
PBE0	0.215 (0.132)	0.212 (0.125)	0.031 (0.026)
DMC: 0.100 (0.043)			
tetramer			
PBE	-0.163 (0.231)	0.230 (0.143)	0.110 (0.070)
BLYP	0.861 (0.392)	1.331 (0.335)	-0.041 (0.036)
B3LYP	0.709 (0.219)	0.859 (0.206)	-0.019 (0.025)
PBE0	0.272 (0.126)	0.282 (0.119)	0.056 (0.038)
DMC: 0.105 (0.044)			
pentamer			
PBE	-0.153 (0.282)	0.276 (0.125)	0.156 (0.077)
BLYP	1.191 (0.335)	1.703 (0.215)	-0.101 (0.050)
B3LYP	0.902 (0.168)	1.060 (0.152)	-0.056 (0.035)
PBE0	0.297 (0.121)	0.304 (0.131)	0.075 (0.042)
DMC: 0.154 (0.046)			
hexamer			
PBE	-0.068 (0.266)	0.318 (0.134)	0.178 (0.077)
BLYP	1.298 (0.376)	1.754 (0.304)	-0.107 (0.053)
B3LYP	0.989 (0.180)	1.123 (0.175)	-0.058 (0.037)
PBE0	0.367 (0.114)	0.367 (0.112)	0.088 (0.041)
DMC: 0.183 (0.044)			

Table 4: Deviations of energies given by corrected DFT approximations away from CCSD(T) benchmark energies for thermal samples of  $(\text{H}_2\text{O})_n$   $3 \leq n \leq 6$  configurations. Notations DFT, DFT- $\Delta_1$  and DFT- $\Delta_{12}$  indicate DFT approximations uncorrected, corrected for 1-body errors, and corrected for both 1- and 2-body errors. Each entry gives the mean deviation, with rms fluctuation of the deviation in parentheses. Mean and rms deviations of DMC energies away from CCSD(T) benchmarks are shown for comparison. Energy units:  $mE_h$  per water monomer.

method	prism	cage	book	ring
MP2	0.00	0.08	0.51	1.84
MP2 <sup>†</sup>	0.00	0.10	0.53	1.93
CCSD(T)	0.00	0.39	1.12	2.70
CCSD(T) <sup>†</sup>	0.00	0.40	1.15	2.87
DMC	0.00	0.53	0.90	2.45
PBE	0.00	-0.55 (-0.95)	-1.99 (-3.14)	-1.45 (-4.32)
PBE- $\Delta_{12}$	0.00	0.00 (-0.40)	-0.78 (-1.93)	-0.20 (-3.07)
PBE- $\Delta_{123}$	0.00	0.35 (-0.05)	1.34 (0.19)	3.16 (0.29)
BLYP	0.00	-0.94 (-1.34)	-3.47 (-4.62)	-3.90 (-6.77)
BLYP- $\Delta_{12}$	0.00	0.04 (-0.36)	0.47 (-0.68)	2.64 (-0.23)
BLYP- $\Delta_{123}$	0.00	0.01 (-0.39)	0.22 (-0.93)	1.72 (-1.15)
B3LYP	0.00	-0.69 (-1.09)	-2.65 (-3.80)	-2.98 (-5.85)
B3LYP- $\Delta_{12}$	0.00	0.05 (-0.35)	0.41 (-0.74)	2.17 (-0.70)
B3LYP- $\Delta_{123}$	0.00	0.04 (-0.36)	0.49 (-0.66)	2.04 (-0.83)
PBE0	0.00	-0.45 (-0.85)	-1.76 (-2.91)	-1.65 (-4.52)
PBE0- $\Delta_{12}$	0.00	0.13 (-0.27)	0.04 (-1.11)	0.96 (-1.91)
PBE0- $\Delta_{123}$	0.00	0.30 (-0.10)	1.21 (0.06)	2.92 (0.05)

Table 5: Total energies of selected isomers of the water hexamer relative to that of the prism, calculated by different methods. In all cases, the geometry of the isomer is the relaxed geometry given by MP2 calculations with the AVTZ basis, as given in the Supplementary Information of Ref. [61]. All energies were calculated in the present work, except for the MP2 and CCSD(T) energies marked with <sup>†</sup> from Ref. [37] and the DMC energies from Ref. [61]. Entries DFT- $n$  with  $n = 2$  and  $3$  are DFT energies corrected for 1- and 2-body errors, and corrected for 1-, 2- and 3-body errors respectively. Values in parentheses represent errors compared with the CCSD(T) energies from Ref. [37]. Energy units:  $mE_h$ .

## Figures

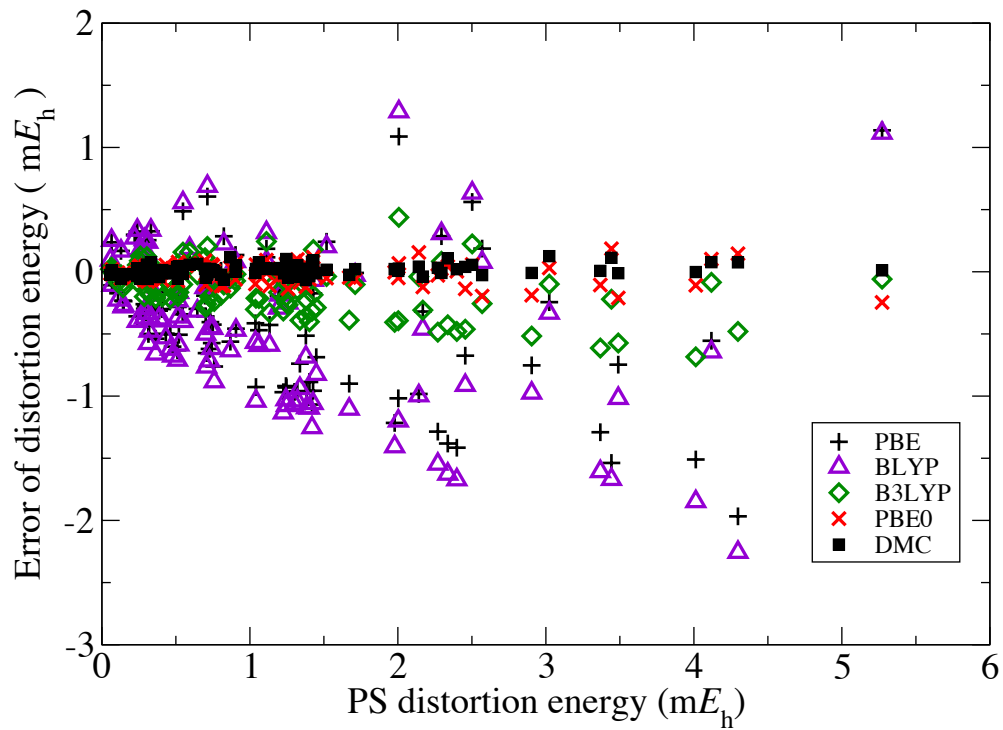


Figure 1: Errors of DFT and DMC distortion energy of the  $H_2O$  monomer for a thermal sample of 100 configurations (see text). Quantities shown are deviations of calculated energies from Partridge-Schwenke (PS) benchmark values with PBE (black pluses), BLYP (purple triangles), B3LYP (green diamonds) and PBE0 (red crosses) and with DMC (black squares) plotted against the PS distortion energy itself. Units:  $mE_h$

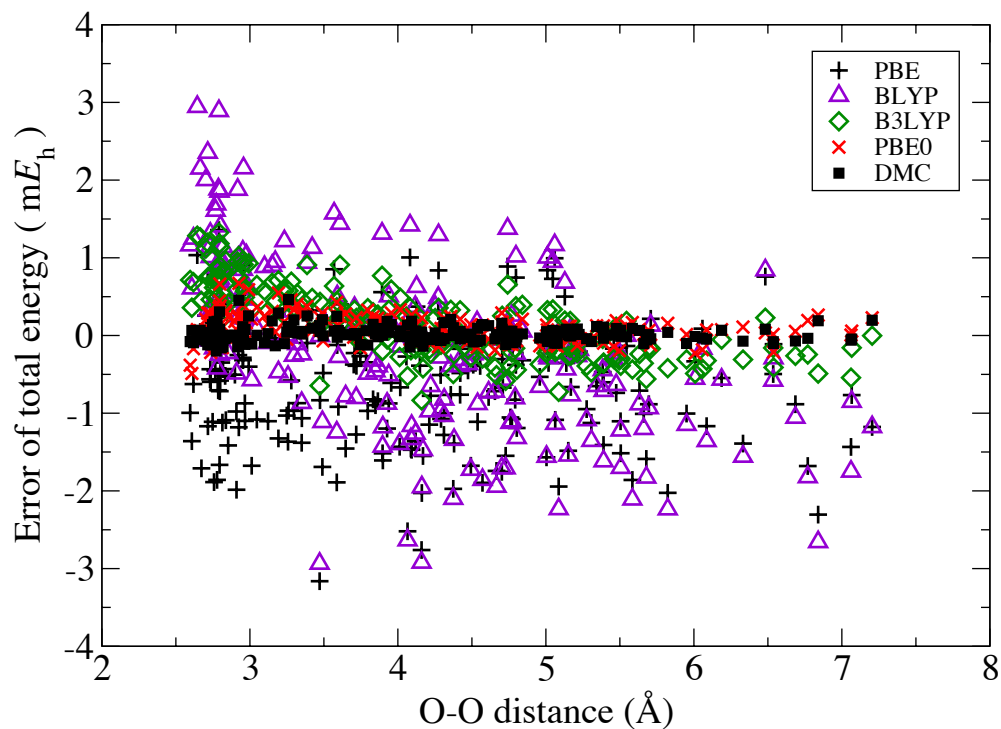


Figure 2: Errors of DMC and DFT approximations relative to CCSD(T) benchmarks for total energies of thermal sample of 198 dimer configuration, plotted vs O-O distance. Symbols represent PBE (black pluses), BLYP (purple triangles), B3LYP (green diamonds) and PBE0 (red crosses) and DMC (black squares). Units:  $mE_h$ .

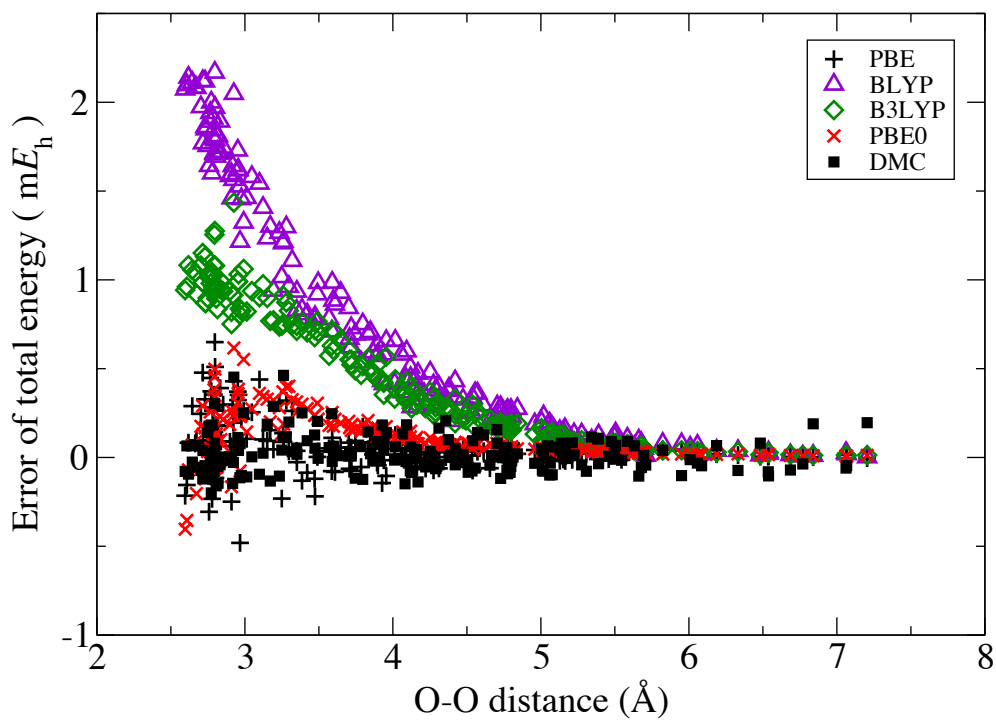


Figure 3: Errors of DFT approximations for total energies of thermal sample of 198 dimer configurations when 1-body part is corrected by replacing the DFT 1-body energy by the essentially exact Partridge-Schwenke function. As in Fig. 2, errors are relative to CCSD(T) benchmarks and are plotted vs O-O distance. Symbols represent PBE (black pluses), BLYP (purple triangles), B3LYP (green diamonds) and PBE0 (red crosses). Errors of DMC (black squares) are shown for comparison. Units:  $mE_h$ .

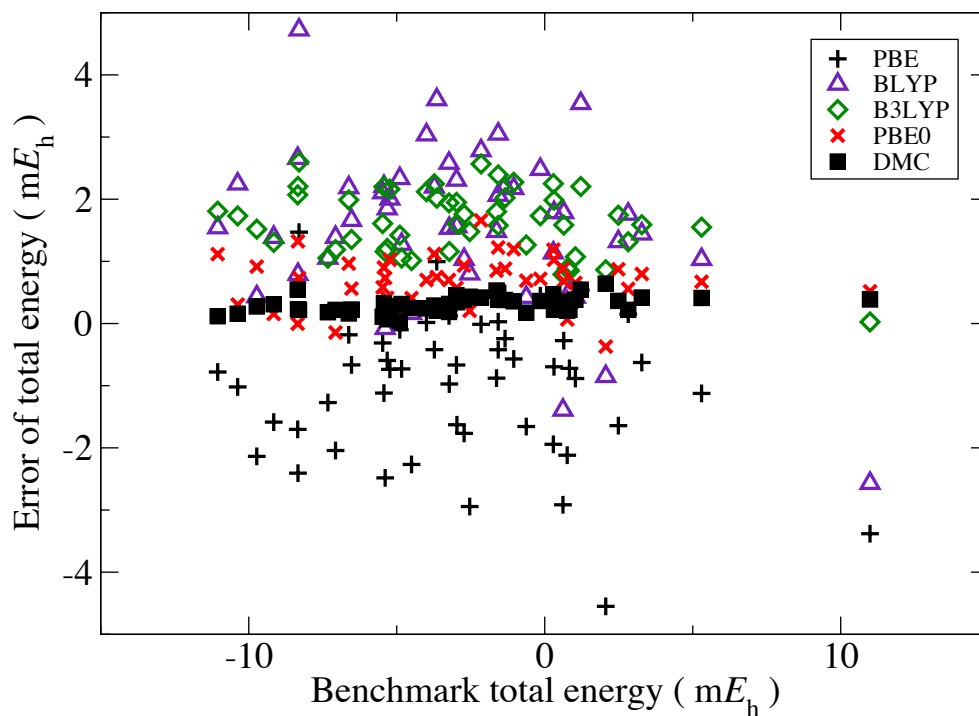


Figure 4: Errors of DFT and DMC total energy of the  $\text{H}_2\text{O}$  trimer for a thermal sample of 50 configurations drawn from a classical simulation of liquid water (see text). Quantities shown are deviations of calculated energies from CCSD(T) benchmark energies near the basis-set limit, with PBE (black pluses), BLYP (purple triangles), B3LYP (green diamonds) and PBE0 (red crosses) and with DMC (black squares) plotted against the benchmark energy itself. Units:  $mE_h$



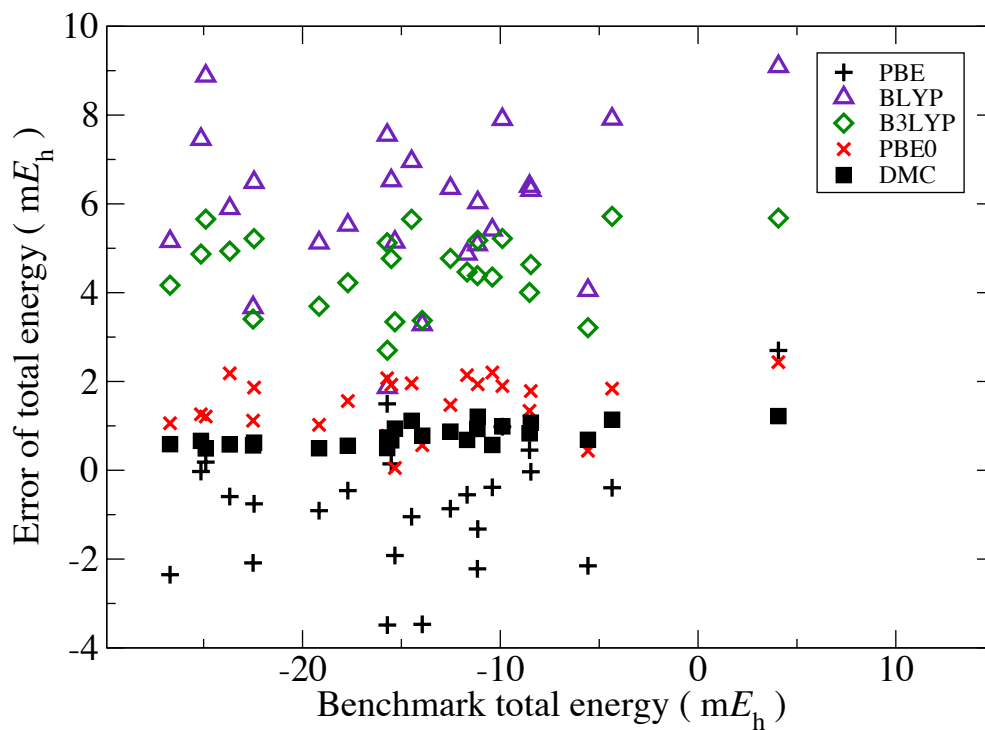


Figure 5: Errors of DFT and DMC total energy of the  $\text{H}_2\text{O}$  pentamer for a thermal sample of 25 configurations drawn from a classical simulation of liquid water (see text). Quantities shown are deviations of calculated energies from CCSD(T) benchmark energies near the basis-set limit, with PBE (black pluses), BLYP (purple triangles), B3LYP (green diamonds) and PBE0 (red crosses) and with DMC (black squares) plotted against the benchmark energy itself. Units:  $mE_h$

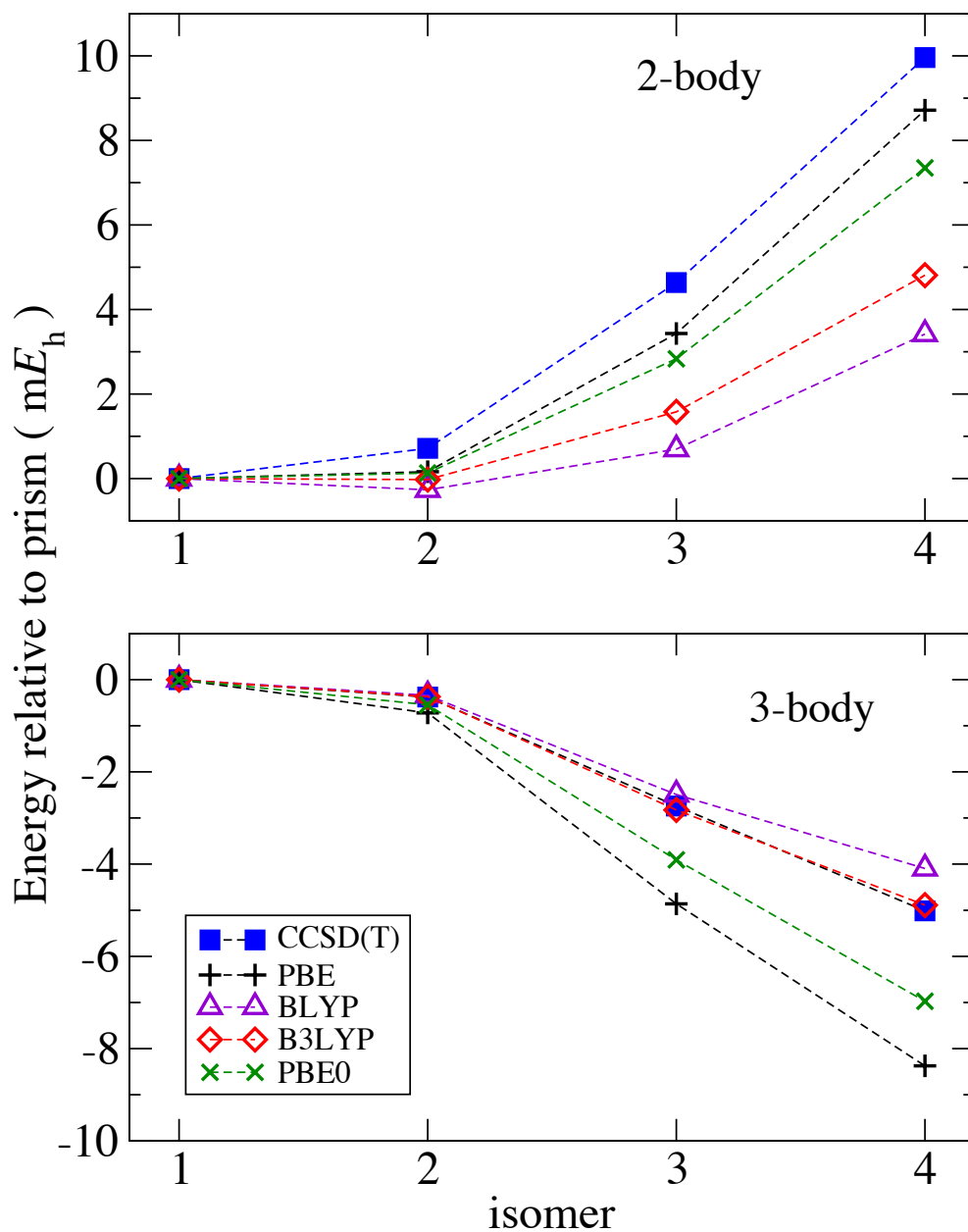


Figure 6: Comparison of DFT values of 2-body energies (upper panel) and 3-body energies (lower panel) of four isomers of the H<sub>2</sub>O hexamer with benchmark values from CCSD(T). Numbering of isomers is prism: 1, cage: 2, book: 3, ring: 4. Units: mE<sub>h</sub>